Killer Toxin K28 resistance in yeast relies on COG complex mediated trafficking of the defence factor Ktd1

Kamilla ME. Laidlaw[1], Hatwan H. Nadir[1], Amy Milburn[1], Martha S.C. Xelhuantzi[1], Justas Stanislovas[1], Alastair P. Droop[2], Sandy MacDonald[2], Ilya Andreev[3], Andrew Leech[2], Dani Ungar[1], Meru Sadhu[3], Chris MacDonald[1,4]

[1] *York Biomedical Research Institute and Department of Biology, University of York, York, UK*
[2] *Bioscience Technology Facility, Department of Biology, University of York, UK*
[3] *Computational and Statistical Genomics Branch, National Human Genome Research Institute, NIH, Bethesda, MD 20892*
[4] *Correspondence: Email: chris.macdonald@york.ac.uk Tel: +44 (0) 1904 328 609*

ABSTRACT

A/B toxins are a diverse family of protein toxins that enter host cells by endocytosis and trigger cell death. In yeast, the killer toxin K28 is an A/B family member that is internalised to endosomes of susceptible host yeast, where the toxin follows the retrograde trafficking pathway and ultimately induces cell cycle arrest. Yeast cells that express the endolysosomal Ktd1 defence factor are protected from K28 toxicity, but modes of Ktd1 regulation are not understood. The COG complex is a conserved tethering complex that is involved in membrane trafficking at the Golgi. Previous research implicated Cog7, a subunit of the COG complex, in K28 defence, but the mechanism is unknown. We employed a high throughput K28 sensitivity assay and bespoke analysis package to show that all lobe B subunits (Cog5 - 8) are required for K28 resistance. Deletion of Golgi localised glycosyltransferase enzymes provides resistance to K28, as cells lack the glycosylated surface proteins required for K28 binding and entry. Although the COG complex modulates glycosylation of surface molecules, our experiments reveal that the hypersensitivity of *cog* mutants is not due to changes in K28 binding but to defects in intracellular trafficking. Ktd1 is mis-localised in *cog* mutants, with a trafficking defect that parallels similar disruptions observed with Snc1, a surface cargo protein that is dependent on the COG complex for recycling via the Golgi. These findings suggest that the COG complex ensures proper trafficking of Ktd1 to endolysosomal compartments, where it can effectively neutralise K28. We propose a model whereby Ktd1 needs to be precisely localised to survey endolysosomes and effectively mediate K28 defence. This work underpins the importance of Ktd1 in defence against the A/B toxin K28, and implies various membrane trafficking regulators might regulate toxin effects in other eukaryotic systems.

INTRODUCTION

Protein toxins are molecular weapons secreted by cells to target other organisms, playing a key role in evolutionary processes (Stern, 2013). Toxins of the A/B family, which includes cholera, Shiga, diphtheria, and ricin, are secreted by diverse organisms and target specific host cells to initiate cell death, through different modes of action (Odumosu et al., 2010). Despite this, most A/B toxins also share various features, such as a bipartite structure consisting of two moieties: an enzymatic active A subunit and a B subunit responsible for binding host cells, although subunit numbers can vary (Márquez-López and Fanarraga, 2023). A/B toxins bind host cells and enter via endocytosis, where the toxin molecules are internalised to endosome compartments before trafficking through the retrograde pathway and triggering cell death (Falnes and Sandvig, 2000).

The yeast Killer Toxin 28 (K28) is a member of the A/B toxin family that is produced by yeast cells infected with the dsRNA M28 virus (Schmitt and Tipper, 1990). K28 is synthesised as a pre-protoxin, and is modified and processed during trafficking through the secretory pathway *en route* to the plasma membrane for secretion (Breinig et al., 2006). Secreted K28 toxin binds to glycosylated residues on the surface of host cells and then enters the cell using canonical endocytic machinery (Eisfeld et al., 2000; Schmitt and Radler, 1987). Internalised K28 traffics from endosomes through the retrograde pathway, ultimately translocating to the nucleus via the cytoplasm to induce G1/S cell cycle arrest (Schmitt et al., 1996).

Ktd1 (Killer toxin defence factor 1) is a membrane protein that localises to the endolysosomal system in yeast and provides resistance to K28 (Andreev et al., 2023). Ktd1 is a member of the Dup240 gene family, which have two transmembrane domains, and mainly localises to the limiting membrane of the vacuole, but is

also found in other endolysosomal compartments. The related tetraspan Cos proteins in the Dup380 family evolved from the same ancestral gene (Despons et al., 2006) but do not localise to the vacuolar membrane, instead sorting proteins and lipids into the multivesicular body pathway for degradation in the lumen of the vacuole (MacDonald et al., 2015a; MacDonald et al., 2015b). Despite its critical role in K28 defence, the mechanism by which Ktd1 protects cells from toxin remains unknown.

The COG complex is a conserved multi-subunit complex that is involved in tethering retrograde vesicles at the Golgi through coordination of soluble NSF (N-ethylmaleimide sensitive factor) attachment proteins (SNAP) receptor (SNARE) mediated membrane fusion (Blackburn et al., 2019). As such, the COG complex is responsible for organisation of Golgi localised glycosylation enzymes that modify transiting glycoproteins. Defects in this processing are associated with a variety of human diseases, including congenital disorders of glycosylation and neurological disorders (Foulquier, 2009). The yeast COG complex is composed of eight subunits (Cog1 - 8) that form two subcomplexes, Cog1 - 4 (lobe A) and Cog5 - 8 (lobe B). One subunit of the COG complex has been implicated in K28 sensitivity, as a genetic screen for mutants with altered response to K28 revealed that *cog7*Δ cells are hypersensitive (Carroll et al., 2009). Whether the role of Cog7 is related to maintenance of the Golgi structure, proper modification of glycosylated K28 binding surface proteins, coordination of proteins transiting the Golgi, or an alternative mechanism is not known. Intriguingly, the genetic screen that implicated Cog7 in K28 defence tested various other mutants of other COG complex and did not find any with altered sensitivity to toxin.

In this study we explore the role of the COG complex in K28 resistance, describe a more sensitive and higher throughput assay to measure growth of yeast exposed to media ± K28 toxin, and propose a model for Ktd1-medated defence that relies on precise membrane trafficking.

RESULTS

The COG complex is implicated in K28 toxin defence

A previous genetic screen for killer toxin K28 sensitive and resistant mutants (**Figure 1A**) was performed using a 96-well based 'halo' assay from a spot of killer toxin secreting cells placed on a lawn of tester strains (Carroll et al., 2009). This screen identified *cog7*Δ mutants as hyper sensitive to K28. To test whether this effect was specific to mutations in *COG7* or more generally through abrogation of the COG complex, we validated null mutants of the non-essential lobe B subunits: *cog5*Δ, *cog6*Δ, *cog7*Δ, *cog8*Δ (**Figure 1B**). Mutants of lobe B have previously been reported to exhibit a growth defect at elevated temperature (Gao and Banfield, 2020; Sinha et al., 2008). All lobe B *cog* mutants grow poorly at of 37°C when compared to wild-type (WT) cells (**Figure 1C**), although this effect was only observed when cells were grown on rich media, with no obvious differences in synthetic complete (SC) minimal media (**Figure 1D**). Although wild-type cells have reduced ability to grow when at elevated temperature on media with alkaline pH, we find this combination is particularly detrimental for growth of the non-essential COG complex mutants. As a control for perturbation of glycosylation, no defects were observed at elevated temperature for *mnn2*Δ mutants, which lack the Golgi resident Alpha-1,2-mannosyltransferase Mnn2 (Raschke et al., 1973; Rayner and Munro, 1998). Mutants of essential lobe A *cog* mutants, with either reduced expression of different *COG* genes by mRNA perturbation (Breslow et al., 2008) or attenuated promoter expression (Arita et al., 2021), failed to phenocopy lobe B *cog* null growth defects at 37°C (**Figure 1E**).

The halo phenotype generated on a lawn of yeast cultured in the presence of K28 secreting cells has a relatively low dynamic range. Before assessing K28 sensitivity of non-essential *cog* mutants we first optimised the halo assay for maximum halo size produced from *ktd1*Δ cells, which are hypersensitive due to the loss of the Ktd1 defence factor (Andreev et al., 2023). High density of cultures used to create lawns correlates with reduced halo size, with the optimal OD_{600} = 0.1 - 0.2 (**Figure 2A**). Next, the culturing media, of both the lawn but also the K28 secretor strain, were tested for effects on halo radius. For this, wild-type (BY4741 and BY4742) and hypersensitive (*ktd1*Δ) lawn strains were grown in rich (YPD) and minimal (SC) media, with and without gelatin, a stabilisation component included in some media recipes for K28 sensitivity (Andreev et al., 2023). Although the difference between media with and without gelatin was not significant, we consistently observed lawns grown in minimal media had larger halos than rich media (**Figure 2B**). Oppositely, we find the K28 secretor strain produces larger halos when grown in YPD. We used these optimised conditions to test K28 sensitivity to lobe B *cog* mutants. As a control for toxin sensitivity, alongside WT cells, we also include *mnn2*Δ, which are resistant to K28 due to reduced binding of K28 (Andreev et al., 2023; Carroll et al., 2009). This assay showed that *cog5*Δ, *cog6*Δ, *cog7*Δ, and *cog8*Δ mutants exhibit a significant increase in K28 sensitivity (**Figure 2C**), with all mutants showing similar levels of sensitivity. This suggests that beyond the additional finding that Cog7 is involved in K28 sensitivity, that the general functionality of the COG complex is required for maintaining resistance to K28 toxicity. However, the *cog* mutants of lobe A mutants did not result in K28 sensitivity (**Figure**

2D). We conclude that the reduced expression of essential lobe A *cog* mutants does not reduce cellular levels of the COG complex sufficiently to inhibit its capacity to tolerate heat stress or K28 exposure.

Cog mutants are hypersensitive to K28

The low sensitivity of the K28 halo assay might explain why only one of four tested *cog* mutants represented in the deletion libraries were identified in a systematic screen (Carroll et al., 2009). Even with optimisation there is relatively little difference between halo radii from wild-type, resistant and sensitive strains. We have recently optimised a liquid plate growth assay that allows more subtle phenotypes to be observed (Andreev et al., 2023). This assay cultures cells in a microtiter plate and monitors growth over time in media enriched with K28 from a hypersecretor strain, compared with control media from a heat cured strain. To analyse data generated from these K28 sensitivity-based growth assays, we have created a bioinformatic analysis pipeline for 96 well plate liquid cultures to document growth curves (**Figure 3A**). This optimised R:Shiny app is available at https://shiny.york.ac.uk/bioltf/cm_growthcurves/. Data comparisons between strains and across different conditions, such as K28 presence are generated, in addition to statistical analyses (**Figure 3B - 3C**). This provides a sensitive and high-throughput analysis pipeline for these K28 assays and could be used for a wide array of applications. We do note that highly resistant strains like mutants with abrogated glycosylation profiles (*mnn1*Δ, *mnn2*Δ, *mnn9*Δ) do exhibit very obvious phenotypes with the halo assay due to essentially having zero growth inhibition (**Figure 3D - 3E**). We compared these mutants in the high throughput liquid plate assay shows very little difference to wild-type cells expressing *KTD1*, which tolerate toxin (**Figure 3E - 3H**). We conclude that both assays have merits, with the halo and liquid based assays being better for assessing resistance and sensitivity phenotypes, respectively. We then used the liquid assay to measure sensitivity of *cog5*Δ, *cog6*Δ, *cog7*Δ, *cog8*Δ mutants. In agreement with the halo-based previous experiments, all lobe B *cog* mutants grow at very similar to wild-type cells over 32-hours in control media lacking K28, but show a significant sensitivity in media containing K28 (**Figure 4A - 4D**). This further supports the notion that a function related to the COG complex, and not an individual subunit, is required for K28 defence.

K28 binding to *cog* mutants is unaffected

These results suggest that the COG complex is required for defence against K28, but the mechanism is unclear. The COG complex in yeast regulates glycosylation of proteins that traffic through the secretory pathway (Fotso et al., 2005; Suvorova et al., 2002; Whyte and Munro, 2001). As mentioned, yeast cells lacking mannosyltransferases, like *mnn2*Δ mutants, are resistant to toxin through reduced capacity for the toxin to bind and enter the cell (Carroll et al., 2009). We hypothesised that deregulation of Golgi mannosyltransferases in *cog* mutants might alter their surface glycosylation profile to increase toxin binding, and therefore explain K28 hypersensitivity (**Figure 5A**). To test this hypothesis, we first created a series of double mutants combining non-essential *cog*Δ deletions with *mnn9*Δ, which lacks the early acting alpha-1,6-mannosyltransferase involved in protein N-linked glycosylation (Gopal and Ballou, 1987; Yip et al., 1994). These mutants are resistant to K28, excluding the possibility that an indirect function of the COG complex explains the K28 sensitive phenotype (**Figure 5B**). We next performed adsorption assays to analyse how well K28 is binds to WT and *cog* mutants (**Figure 5C**). This data included a *mnn2*Δ control that does not efficiently bind K28. These experiments showed no significant changes in the ability of K28 to bind *cog* mutant cells (**Figure 5D**). We predicted that adsorption of K28 in all four lobe B *cog* mutants would need to be obvious to explain their high sensitivity to K28 phenotype.

The COG complex is required for proper vacuolar sorting of Ktd1

As elevated adsorption does not explain *cog* mutant K28 sensitivity, we explored other explanations. Although the COG complex does coordinate Golgi enzymes, it achieves this through a fundamental regulation of membrane trafficking at the Golgi (Blackburn et al., 2019). It has been previously shown that yeast synaptobrevin, a SNARE protein that localises mainly to the surface, is mis-localised in *cog* mutant cells (Whyte and Munro, 2001), likely as Snc1 recycles via the Golgi in a ubiquitin dependent manner (Laidlaw et al., 2022; Xu et al., 2017). We expressed GFP-Snc1 in *cog5*Δ, *cog6*Δ, *cog7*Δ, *cog8*Δ mutant strains and confirmed that all exhibit severe mis-localisation phenotypes, unlike wild-type and *mnn2*Δ cells, which correctly localise Snc1 to the surface in a polarised manner (**Figure 5A**). We note that in addition to various bright punctate GFP-Snc1 spots in the lobe B *cog* mutants, but there is also GFP signal in the vacuolar lumen. Indeed, there is also fragmented vacuolar phenotype indicated with CMAC staining in the mutant strains. As these mutants disrupt trafficking of post-Golgi cargoes, we next asked whether they also mis-localises the K28 toxin defence factor Ktd1. As expected, GFP-Ktd1 localises to the vacuole membrane in wild-type and *mnn2*Δ cells. However, in lobe B *cog* complex mutants, GFP-Ktd1 has a severe mis-localisation phenotype. Although some GFP-Ktd1 signal is found at the vacuolar membrane, there are many aberrant localisations, which includes large intracellular aggregates and signal at the endoplasmic reticulum. We conclude that the primary role for the COG complex in K28 toxin defence is coordinating precise endolysosomal trafficking of the membrane protein Ktd1.

DISCUSSION

This study investigates the role of the COG complex in yeast resistance to the Killer Toxin 28 (K28) and provides evidence that its function is essential for proper trafficking of the K28 defence factor Ktd1 to post-Golgi endolysosomal compartments. Our findings extend the current understanding of how intracellular trafficking contribute to cellular resistance against toxins of the A/B family.

Our study confirms and expands upon previous observations implicating the COG complex in K28 toxin sensitivity. Specifically, we show that deletion of non-essential lobe B subunits of the COG complex (Cog5–8) results in a significant increase in K28 sensitivity. This suggests that the functional integrity of the entire lobe B subcomplex is critical for toxin defence and may have unique functional role in K28 defence that is distinct from the canonical functions of the COG complex. Alternatively, the entire COG complex is required for mediating efficient defence against K28 and the essentiality of the lobe A mutants make functional testing of those subunits uninformative; we speculate the latter is most likely. We tested various mutant alleles of the essential lobe A subunits, with reduced levels of different subunits, but these failed to show phenotypes when tested at elevated temperature or following exposure to K28 (**Figure 1E, 2D**). While prior studies identified Cog7 as being important for K28 resistance (Carroll et al., 2009), our data demonstrate that the other lobe B subunits are equally critical. We speculate that although the previous genetic screen was performed in an extremely robust manner, with mutants being validated extensively, the screen suffered from the relatively low resolution 'halo' based assay, which is particularly difficult to perform at scale.

This prompts considerations of assays for K28 sensitivity. Enriching media with K28 from a diploid hyper-secreting strain, with control media from heat-cured cells that do not secrete K28, is effective in liquid assays (Andreev et al., 2023; Schmitt and Tipper, 1990). Performing these liquid growth measurements at 96-well density increases capacity and our bespoke analysis package generates extensive data, including growth profiles ± K28 toxin and comparisons to reference selected strains (e.g. wild-type cells). However, we also note that wild-type cells - which endocytose and tolerating K28 via Ktd1 - do not have capacity for significantly better growth to entirely resistant strains. Although the halo-based K28 assay does have a small dynamic range to distinguish sensitive, resistant or wild-type phenotypes, we found it very effective at highlighting the differences between wild-type cells and resistant strains, such as those lacking mannosyltransferase (**Figure 3D**). We recommend using both assays in the first instance.

Our hypotheses about the COG complex regulating toxin binding led to some adjacent observations about the role of glycosylation in toxin mediated cell death. Previous studies showing that mannosyltransferase mutants, such as *mnn2*Δ, confer resistance to K28 by reducing toxin binding to the cell surface (Andreev et al., 2023; Carroll et al., 2009). Defects in the COG complex, which results in mis-localisation or degradation of Golgi localised glycosyltransferases, have an impact on glycosylation profiles at the yeast cell surface (Smith and Lupashin, 2008). However, adsorption assays revealed no significant difference in K28 binding between wild-type and all lobe B *cog* mutant cells, and double mutants lacking both COG subunits and *MNN9* exhibited resistance similar to *mnn9Δ* single mutants (**Figure 5B**). These results strongly suggest that the hypersensitivity of *cog* mutants to K28 is independent of glycosylation-mediated toxin binding.

We next hypothesised that the increased K28 sensitivity in cog mutants could result from defects in intracellular trafficking rather than glycosylation. GFP-Snc1 is known to recycle via the Golgi with steady state localisation at the surface reliant on efficient recycling via endosomally localised COPI and other factors, including the COG complex for proper sorting to post-Golgi compartments (MacDonald and Piper, 2016; Whyte and Munro, 2001). Similarly, we observed severe trafficking defects of GFP-Ktd1 in *cog5Δ, cog6Δ, cog7Δ, and cog8Δ* mutants. Unlike wild-type cells, where Ktd1 localises predominantly to the vacuolar membrane, *cog* mutants exhibit aberrant Ktd1 localisation, including intracellular aggregates and endoplasmic reticulum (ER) accumulation. The steady state mis-localisation phenotype of GFP-Snc1 in *cog* mutants is compounded by multiple rounds of surface recycling via the Golgi (Lewis et al., 2000). Ktd1 localises to early endosomes, multivesicular bodies and the *trans*-Golgi network (Andreev et al., 2023). One interpretation of GFP-Ktd1 also severely mis-localising is Ktd1 may transit these compartments as a toxin surveillance mechanism, which relies on proper membrane trafficking machinery.

The mis-localisation of Ktd1 in *cog* mutants provides a mechanistic explanation for their hypersensitivity to K28. Ktd1 is a key defence factor that localises to the vacuolar membrane, where it likely functions to neutralise internalised K28 toxin or prevent its retrograde trafficking. Disruption of Ktd1 localisation in *cog* mutants would impair its protective function, rendering cells more susceptible to K28-induced cell death. The requirement for the COG complex in trafficking Ktd1 to the vacuolar membrane underscores the importance of membrane trafficking pathways in cellular defence against such toxins. The findings presented here have broader implications for understanding cellular resistance mechanisms against A/B toxins. It is possible that analogous mechanisms involving the trafficking of defence factors may exist in other organisms, including higher eukaryotes. Lysosomes in animal cells swell in response to endocytosed toxin (Turner et al., 2023) and lysosomal degradation of Shiga toxin occurs if retrograde trafficking to the Golgi is blocked (Mukhopadhyay and Linstedt, 2012).

MATERIALS & METHODS

Cell culture

Yeast cultures were typically grown in rich yeast extract peptone dextrose (YPD) medium 2% glucose, 2% peptone, 1% yeast extract or synthetic complete (SC) minimal medium 2% glucose, yeast nitrogen base supplemented with appropriate amino acids and bases. For making agar plates, 2% agar is also added prior to autoclaving. Cells were routinely grown overnight at 30°C with shaking to early/mid-log phase ($OD_{600} \leq 1.0$) prior to experimentation.

Plate based growth assays

Yeast cultures were grown to log phase in SC or YPD media as indicated, then used to create 10-fold serial dilutions in a microtiter plate. Yeast were then sotted on plates, allowed to dry at room temperature and then indicated at indicated temperatures. Growth of plates was then recorded, typically after 24 - 48 hours.

Halo K28 sensitivity assay

Strains for assessment were cultured to saturation overnight, then OD_{600} measurements were used to normalise lawn densities to OD_{600} = 0.1 - 0.2, unless otherwise stated. Lawns were plated on agar media containing phosphate citrate buffer and adjusted to pH 4.7. A *ski2Δ*/*ski2-2* diploid strain infected with the M28 virus was used cultured to log phase (OD_{600} ~ 1.0) before cultures were concentrated 10-fold and 5 - 7 technical repeats per plate spotted on to the lawns. Yeast were grown for 48 hours at room temperature before growth was recorded. Images were contrast adjusted using Fiji/ImageJ and the radii of halos were measured with 4 individual measurements per spot across all technical replicates and data from biological replicates plotted.

Purification of enriched media

K28 toxin secretor cells and a heat-cured negative control strain were grown in SC media pH 4.7 for 48 hours at 23°C with agitation at 70 rpm. The media was then filter sterilised and stored on ice, before addition of 5x concentrated SC media (pH 4.7) to replenish nutrients to the toxin enriched media. Growth of cells was measured using the Clariostar (BMG LabTech) automated plate reader by increase in absorbance at 600 nm in a 96-well plate format containing 200µl of K28 toxin containing, or the heat cured control media. Strains for assessment were cultured to saturation overnight, then ~1.5 µl added to each wells, with between 3 and 56 technical repeats for both K28 and control media. Absorbance measurements were taken every 10 minutes for 27 - 32 hours. Prior to each measurement, the plate underwent orbital shaking for 30 seconds. Raw data was then organised and read with an R:Shiny Package (https://shiny.york.ac.uk/bioltf/cm_growthcurves/) to generate graphs and statistics.

K28 adsorption assays

To test K28 binding to different strains, toxin enriched media was processed as described above before. Strains to be tested were cultured overnight and OD_{600} used to harvest equal amounts of each strain. Pellets were incubated for 15 minutes at 4°C in toxin enriched media, with all comparisons in each biological replicate performed at the same with the same media preparation. Following the adsorption period, cells were removed and the resultant media filtered again and then used in growth assays, also described above, to assay the efficacy of any remaining toxin in the media. Area under the curve following 32 hours growth was normalised to wild-type controls on the day, and then plotted as an indirect measure of toxin in the media.

Confocal microscopy

Wild type and knock out yeast strains expressing GFP-tagged proteins were grown overnight to mid-log phase, and imaged at room temperature using a 63x 1.40 oil immersion Plan Apochromat objective lens on a Zeiss LSM 980 with Airyscan2. GFP fluorescence was excited using a 488 nm Argon laser and 495–550 nm emission collected. Yeast vacuoles were labelled with 50 µM CMAC and washed x3 prior to confocal imaging. Blue fluorescence of CMAC was excited with a 405 nm laser and emissions collected at 422/497 nm.
Processed images were adjusted in Fiji/ImageJ software (NIH).

ACKNOWLEDGMENTS

We would like to thank staff at the York Bioscience Technology Facility for technical assistance. This research was supported by a Sir Henry Dale Research Fellowship from the Wellcome Trust and the Royal Society 204636/Z/16/Z (CM).

CONTRIBUTIONS

Conceptualization: IA, DU, MS, CMD
Methodology: MS, CMD
Software: AD, SM
Validation: KL, HN, AM, MX
Investigation: KL, HN, AM, MX, JS, CMD
Writing - Original Draft: CMD
Writing - Review & Editing: HN, AM, CMD
Resources: AL
Visualization: KL, AD, SM, CMD
Supervision: DU, CMD
Project administration: CMD
Funding acquisition: CMD

DECLARATION OF INTERESTS

The authors declare no competing interests.

FIGURES AND LEGENDS

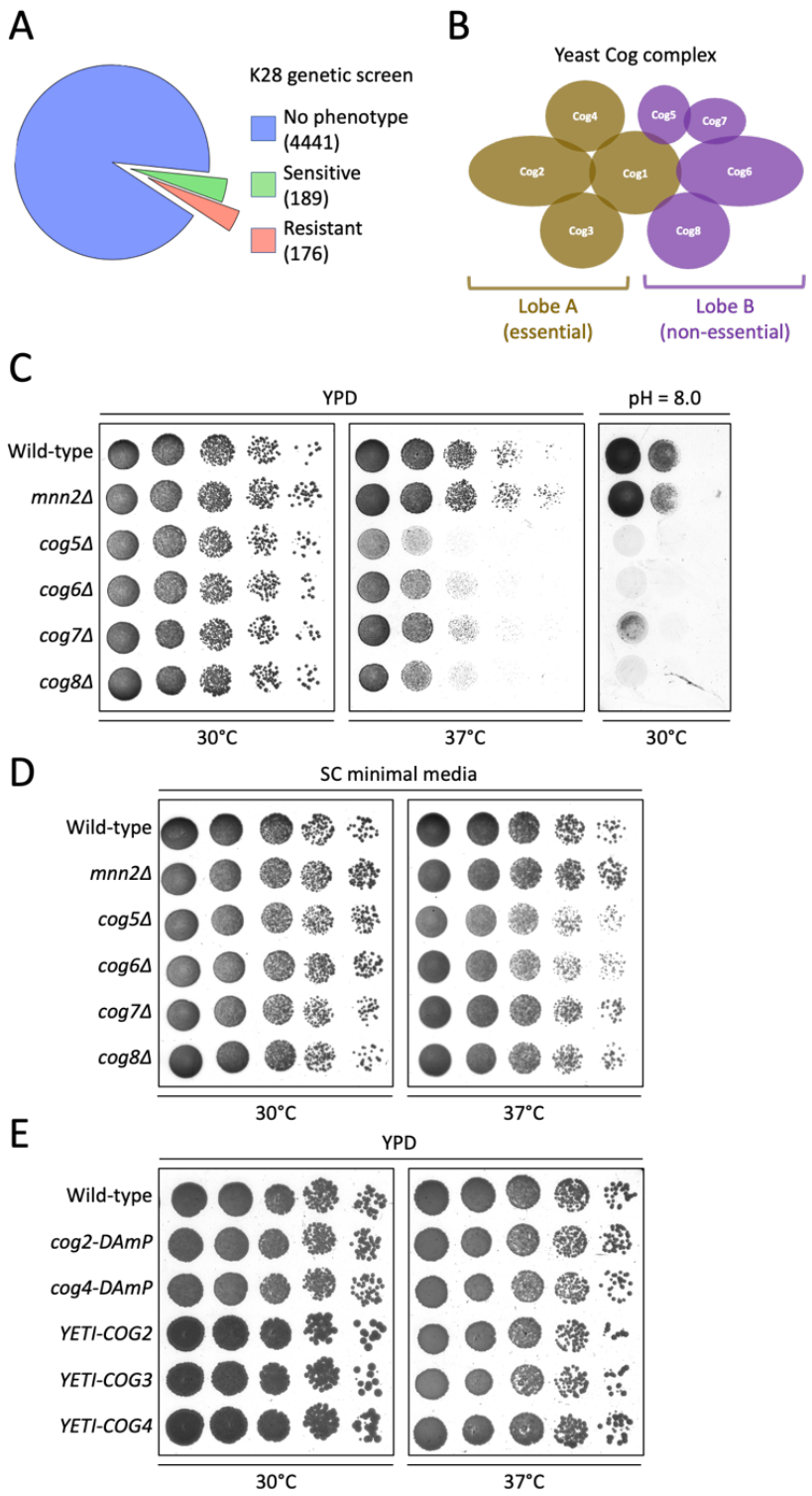

Figure 1: Deletion of non-essential COG complex subunits causes growth defect
A) Summary of K28 sensitivity genetic screen performed by (Carroll et al., 2009), showing mutants tested that have no change upon K28 treatment (blue), hypersensitive (green) and resistant (red) strains.
B) Schematic representation of the yeast Cog complex comprised of 8 subunits organised between Lobe A (Cog1 - 4; yellow) and Lobe B (Cog5 - 8; purple), with some of the main physical interactions depicted with subunit overlap.
C - E) Wild-type (WT) and indicated mutant strains were grown to mid-log phase overnight in YPD media before normalised cell pellets were harvested and diluted 10-fold in water prior to 5µl spotted onto solid agar media: YPD **(C, E)**, or SC **(D)** and incubated at either 30°C or 37°C prior to recording growth.

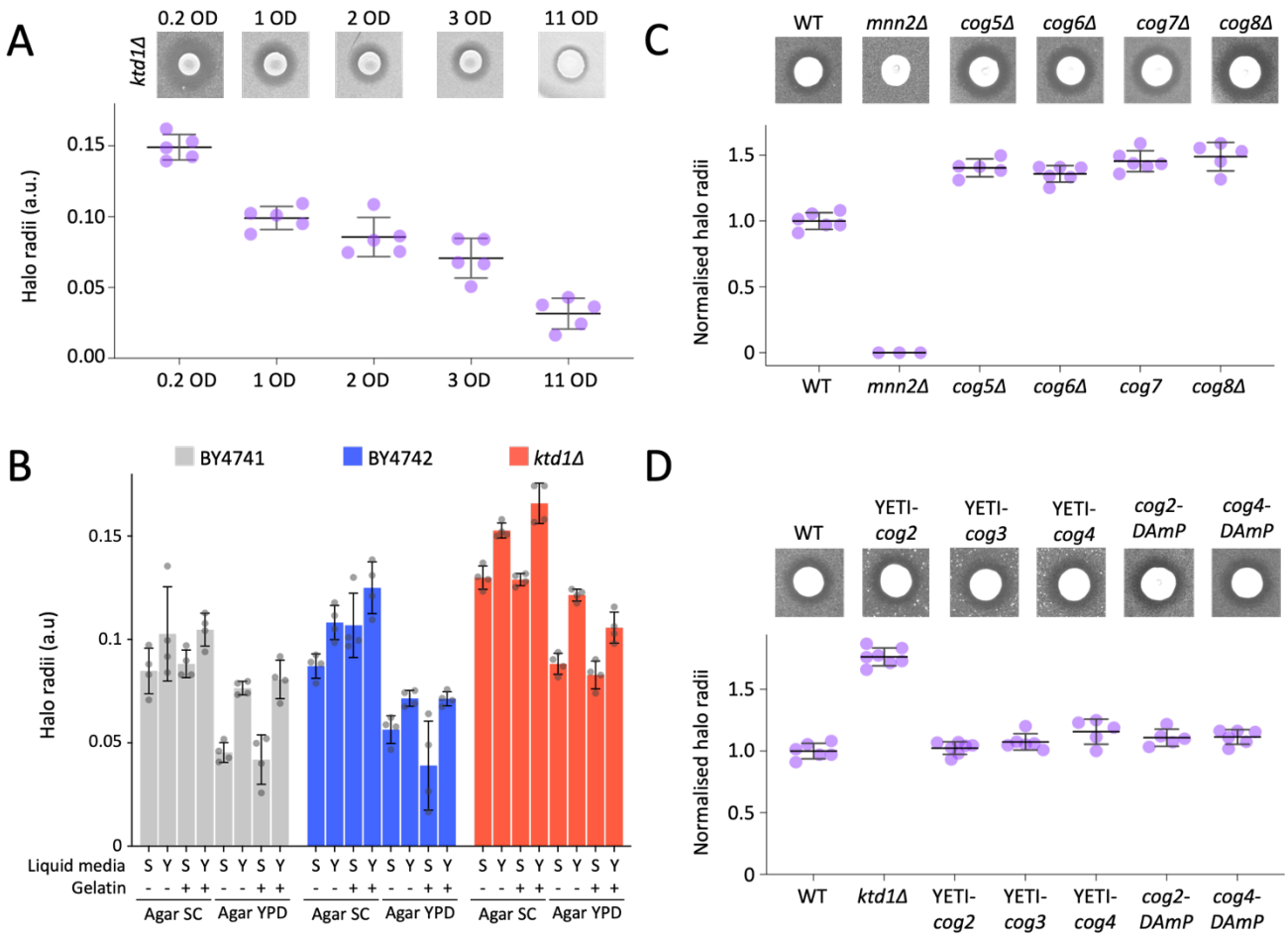

Figure 2: Optimised halo assay shows the COG complex is required for K28 toxin resistance
A) Indicated yeast strains were grown to mid-log phase in SC media before lawns at OD_{600} = 0.1 was spread on a SC pH 4.7 plate before K28 secretor cells added, with representative halos (upper) and quantified biological repeats (n=5).
B) Data from a large series of K28 sensitivity halo assays for two wild-type strains (BY4741 and BY4742) in addition to *ktd1*Δ mutants are plotted. Strains for testing were plated on agar containing either SC or YPD media, with and without type B gelatin for toxin stability. Liquid SC (S) or YPD (Y) media was used to culture the K28 secretor cells.
C - D) K28 sensitivity halo assays were formed with indicated strains with quantified halo radii (n > 3) plotted below.

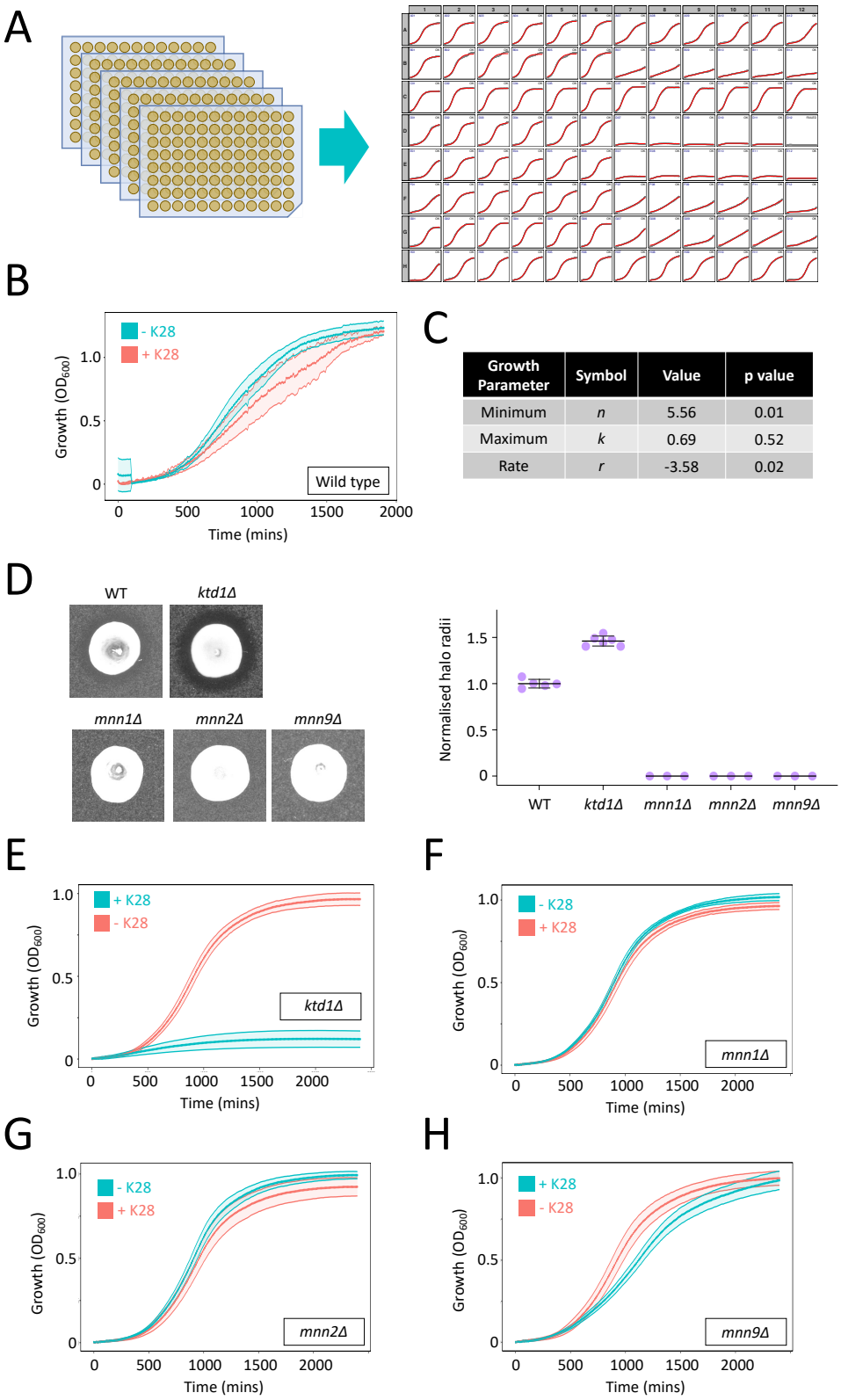

Growth Parameter	Symbol	Value	p value
Minimum	*n*	5.56	0.01
Maximum	*k*	0.69	0.52
Rate	*r*	-3.58	0.02

Figure 3: Analysis pipeline for high-throughput liquid assay
A) A high throughput 96 well plate liquid assay for yeast growth including example plot used for quality control assessment of growth profiles.
B) Growth profile of wild-type cells exposed to media -K28 (blue) or +K28, (red) with standard deviation shown in shaded regions.
C) Growth parameters extracted from the R:shiny app used to generate graphs from raw data imported.
D) Halo assays of indicated lawns exposed to spot of K28 secretor cells, with quantification (n ≥ 3) depicted.
E - H) Liquid growth assays of indicated cells grown in control media (blue) or K28 enriched media (red).

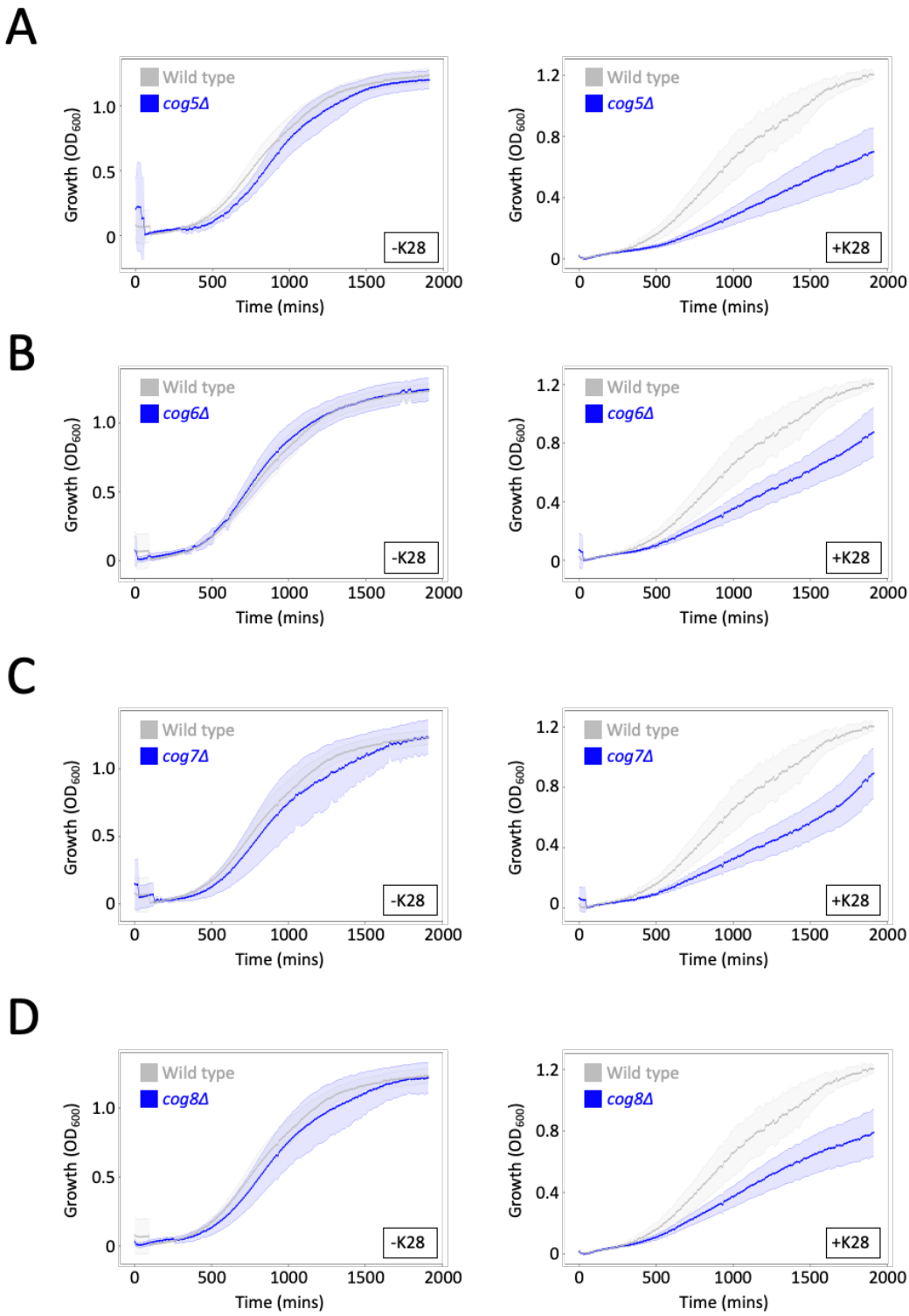

Figure 4: *cog* mutants are hypersensitive to K28 in liquid growth assay.
A - D) Indicated *cog* mutants (blue) were compared to wild-type cells (grew) grown in same conditions in the same plate, both in media from heat cured yeast (left) and media enriched with active toxin (right).

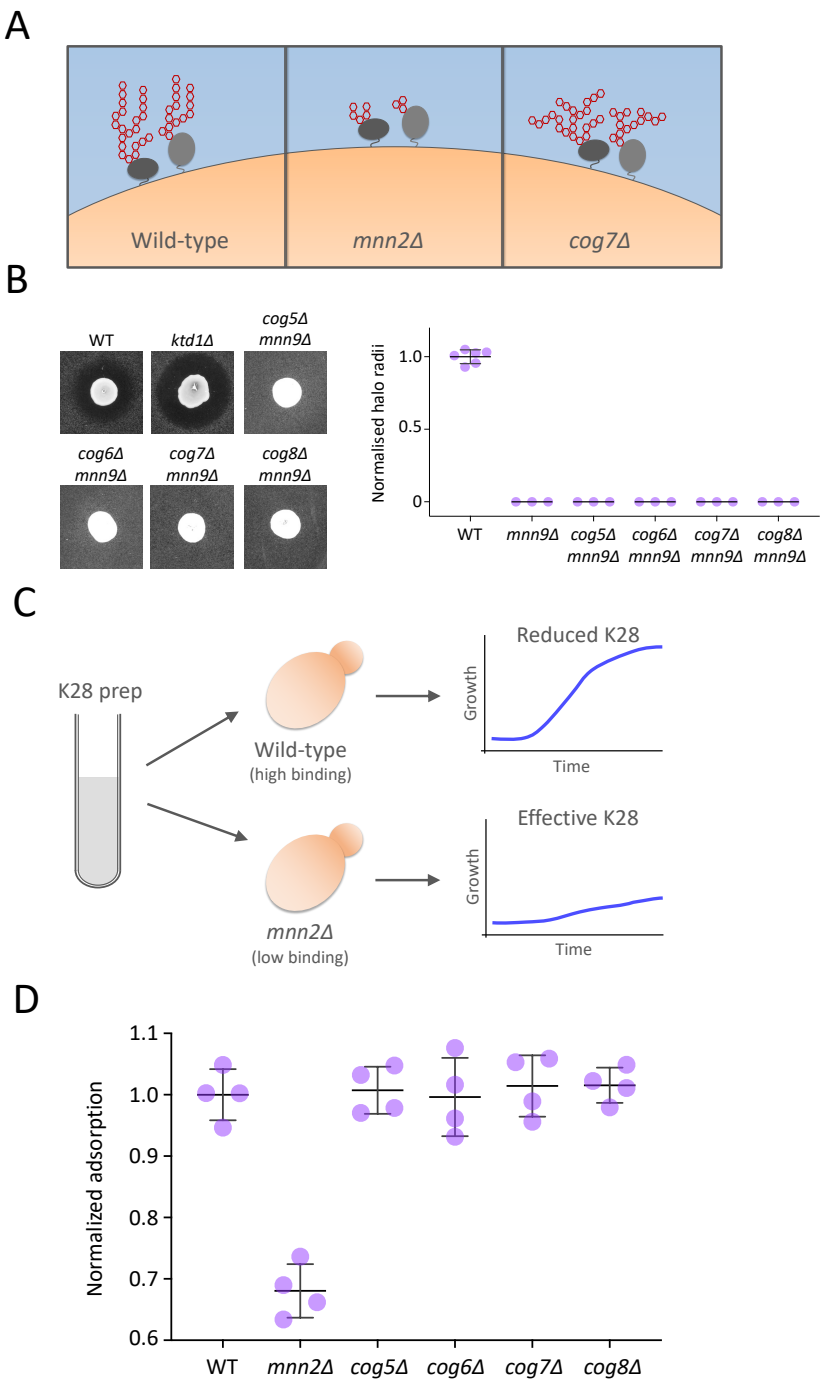

Figure 5: Hypothetical model for COG complex-mediated K28 sensitivities
A) Cartoon model to depict hypothesis that mannosyltransferase mutants like *mnn2*Δ have reduced binding of K28 but that *cog7*Δ cells might have altered glycosylation profiles that have higher toxin affinity.
B) K28 based halo assays for indicated mutants, including quantifications (n ≥ 3).
C) Basis for adsorption assay, where media enriched for toxin is preincubated with tester cells for adsorption, before cells re removed and toxin efficacy in media is tested indirectly by growth capacity of wild-type cells.
D) Adsorption assay results normalised to wild-type cells and compared across indicated strains (n = 4).

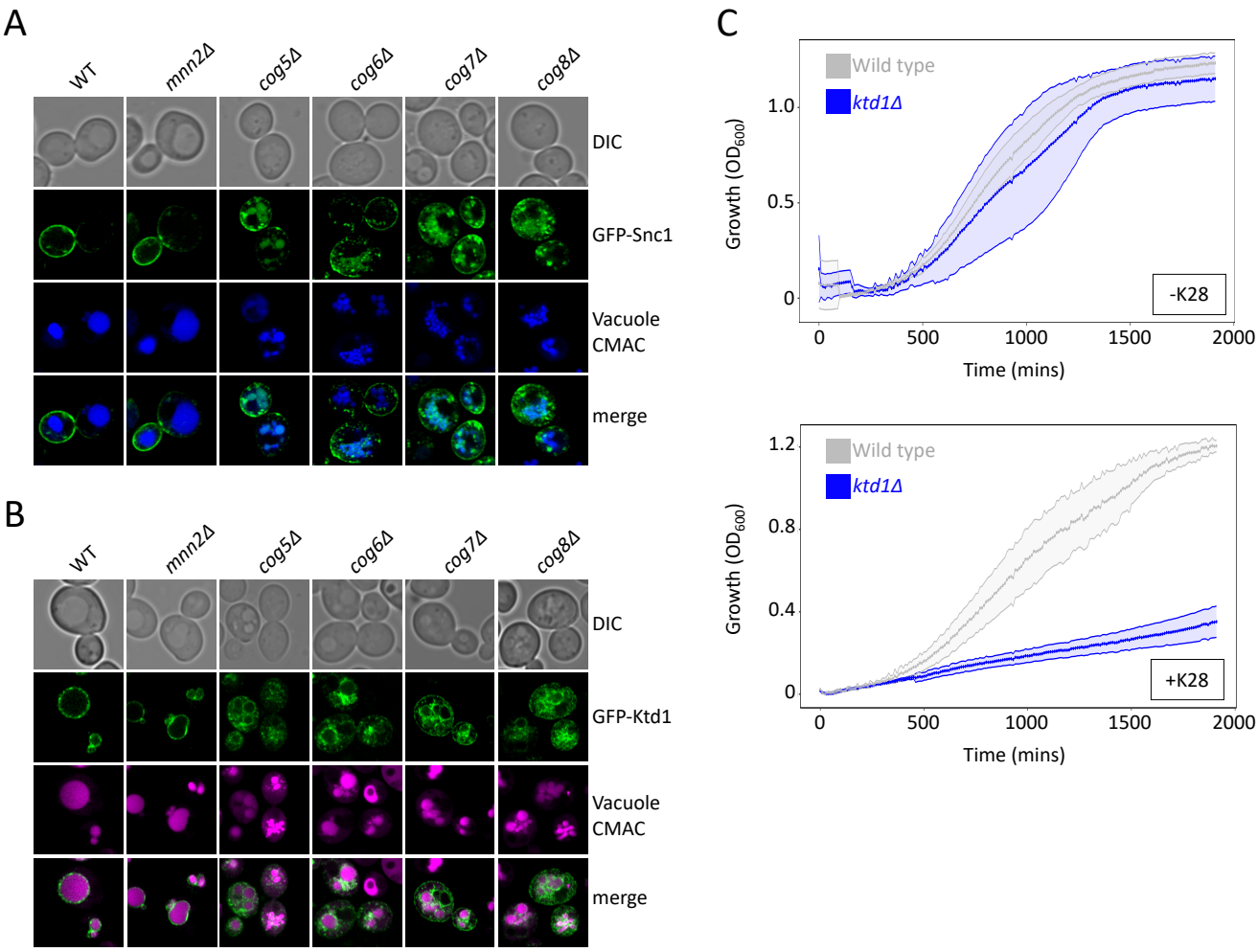

Figure 6: Correct localisation of Ktd1 requires the COG complex
A - B) Indicated strains expressing GFP-Snc1 (A) and GFP-Ktd1 (B) from a plasmid were grown to mid-log phase overnight, vacuoles were stained with CMAC (blue, A; Magenta B)) prior to Airyscan2 confocal microscopy.
C) Growth curves comparing wild-type (grey) and *ktd1*Δ mutants in control media (upper) and active K28 containing media (lower).

REFERENCES

Andreev, I., Laidlaw, K. M. E., Giovanetti, S. M., Urtecho, G., Shriner, D., Bloom, J. S., MacDonald, C. and Sadhu, M. J. (2023). Discovery of a rapidly evolving yeast defense factor, KTD1, against the secreted killer toxin K28. *Proc National Acad Sci* **120**, e2217194120.

Arita, Y., Kim, G., Li, Z., Friesen, H., Turco, G., Wang, R. Y., Climie, D., Usaj, M., Hotz, M., Stoops, E. H., et al. (2021). A genome-scale yeast library with inducible expression of individual genes. *Mol Syst Biol* **17**, e10207.

Blackburn, J. B., D'Souza, Z. and Lupashin, V. V. (2019). Maintaining order: COG complex controls Golgi trafficking, processing, and sorting. *FEBS Lett.* **593**, 2466–2487.

Breinig, F., Sendzik, T., Eisfeld, K. and Schmitt, M. J. (2006). Dissecting toxin immunity in virus-infected killer yeast uncovers an intrinsic strategy of self-protection. *Proc. Natl. Acad. Sci.* **103**, 3810–3815.

Breslow, D. K., Cameron, D. M., Collins, S. R., Schuldiner, M., Stewart-Ornstein, J., Newman, H. W., Braun, S., Madhani, H. D., Krogan, N. J. and Weissman, J. S. (2008). A comprehensive strategy enabling high-resolution functional analysis of the yeast genome. *Nat Methods* **5**, 711–718.

Carroll, S. Y., Stirling, P. C., Stimpson, H. E. M., Gießelmann, E., Schmitt, M. J. and Drubin, D. G. (2009). A Yeast Killer Toxin Screen Provides Insights into A/B Toxin Entry, Trafficking, and Killing Mechanisms. *Dev. Cell* **17**, 552–560.

Despons, L., Wirth, B., Louis, V. L., Potier, S. and Souciet, J.-L. (2006). An evolutionary scenario for one of the largest yeast gene families. *Trends Genet* **22**, 10 15.

Eisfeld, K., Riffer, F., Mentges, J. and Schmitt, M. J. (2000). Endocytotic uptake and retrograde transport of a virally encoded killer toxin in yeast. *Mol. Microbiol.* **37**, 926–940.

Falnes, P. Ø. and Sandvig, K. (2000). Penetration of protein toxins into cells. *Curr. Opin. Cell Biol.* **12**, 407–413.

Fotso, P., Koryakina, Y., Pavliv, O., Tsiomenko, A. B. and Lupashin, V. V. (2005). Cog1p Plays a Central Role in the Organization of the Yeast Conserved Oligomeric Golgi Complex*. *J. Biol. Chem.* **280**, 27613–27623.

Foulquier, F. (2009). COG defects, birth and rise! *Biochim. Biophys. Acta (BBA) - Mol. Basis Dis.* **1792**, 896–902.

Gao, G. and Banfield, D. K. (2020). Multiple features within the syntaxin Sed5p mediate its Golgi localization. *Traffic* **21**, 274–296.

Gopal, P. K. and Ballou, C. E. (1987). Regulation of the protein glycosylation pathway in yeast: structural control of N-linked oligosaccharide elongation. *Proc. Natl. Acad. Sci.* **84**, 8824–8828.

Laidlaw, K. M. E., Calder, G. and MacDonald, C. (2022). Recycling of cell surface membrane proteins from yeast endosomes is regulated by ubiquitinated Ist1. *J Cell Biology* **221**, e202109137.

Lewis, M. J., Nichols, B. J., Prescianotto-Baschong, C., Riezman, H. and Pelham, H. R. (2000). Specific retrieval of the exocytic SNARE Snc1p from early yeast endosomes. *Molecular biology of the cell* **11**, 23 38.

MacDonald, C. and Piper, R. C. (2016). Cell surface recycling in yeast: mechanisms and machineries. *Biochem Soc T* **44**, 474 478.

MacDonald, C., Payne, J. A., Aboian, M., Smith, W., Katzmann, D. J. and Piper, R. C. (2015a). A Family of Tetraspans Organizes Cargo for Sorting into Multivesicular Bodies. *Dev Cell* **33**, 328 342.

MacDonald, C., Stamnes, M. A., Katzmann, D. J. and Piper, R. C. (2015b). Tetraspan cargo adaptors usher GPI-anchored proteins into multivesicular bodies. *Cell Cycle* **14**, 3673 3678.

Márquez-López, A. and Fanarraga, M. L. (2023). AB Toxins as High-Affinity Ligands for Cell Targeting in Cancer Therapy. *Int. J. Mol. Sci.* **24**, 11227.

Mukhopadhyay, S. and Linstedt, A. D. (2012). Manganese Blocks Intracellular Trafficking of Shiga Toxin and Protects Against Shiga Toxicosis. *Science* **335**, 332–335.

Odumosu, O., Nicholas, D., Yano, H. and Langridge, W. (2010). AB Toxins: A Paradigm Switch from Deadly to Desirable. *Toxins* **2**, 1612–1645.

Raschke, W. C., Kern, K. A., Antalis, C. and Ballou, C. E. (1973). Genetic Control of Yeast Mannan Structure ISOLATION AND CHARACTERIZATION OF MANNAN MUTANTS. *J. Biol. Chem.* **248**, 4660–4666.

Rayner, J. C. and Munro, S. (1998). Identification of the MNN2 and MNN5 mannosyltransferases required for forming and extending the mannose branches of the outer chain mannans of Saccharomyces cerevisiae. *J. Biol. Chem.* **273**, 26836–43.

Schmitt, M. and Radler, F. (1987). Mannoprotein of the Yeast Cell Wall as Primary Receptor for the Killer Toxin of Saccharomyces cerevisiae Strain 28. *Microbiology* **133**, 3347–3354.

Schmitt, M. J. and Tipper, D. J. (1990). K28, A Unique Double-Stranded RNA Killer Virus of Saccharomyces cerevisiae. *Mol. Cell. Biol.* **10**, 4807–4815.

Schmitt, M. J., Klavehn, P., Wang, J., Schönig, I. and Tipper, D. J. (1996). Cell cycle studies on the mode of action of yeast K28 killer toxin. *Microbiology* **142**, 2655–2662.

Sinha, H., David, L., Pascon, R. C., Clauder-Münster, S., Krishnakumar, S., Nguyen, M., Shi, G., Dean, J., Davis, R. W., Oefner, P. J., et al. (2008). Sequential Elimination of Major-Effect Contributors Identifies Additional Quantitative Trait Loci Conditioning High-Temperature Growth in Yeast. *Genetics* **180**, 1661–1670.

Smith, R. D. and Lupashin, V. V. (2008). Role of the conserved oligomeric Golgi (COG) complex in protein glycosylation. *Carbohydr. Res.* **343**, 2024–2031.

Stern, D. L. (2013). The genetic causes of convergent evolution. *Nat. Rev. Genet.* **14**, 751–764.

Suvorova, E. S., Duden, R. and Lupashin, V. V. (2002). The Sec34/Sec35p complex, a Ypt1p effector required for retrograde intra-Golgi trafficking, interacts with Golgi SNAREs and COPI vesicle coat proteins. *J. Cell Biol.* **157**, 631–643.

Turner, M., Plumb, J., Merrill, A. R., Grinstein, S. and Westman, J. (2023). Lysosomal swelling and lysis mediate delivery of C3 toxins to their cytoplasmic targets. *Mol. Microbiol.* **119**, 695–710.

Whyte, J. R. C. and Munro, S. (2001). The Sec34/35 Golgi Transport Complex Is Related to the Exocyst, Defining a Family of Complexes Involved in Multiple Steps of Membrane Traffic. *Dev. Cell* **1**, 527–537.

Xu, P., Hankins, H. M., MacDonald, C., Erlinger, S. J., Frazier, M. N., Diab, N. S., Piper, R. C., Jackson, L. P., MacGurn, J. A. and Graham, T. R. (2017). COPI mediates recycling of an exocytic SNARE by recognition of a ubiquitin sorting signal. *Elife* **6**, e28342.

Yip, C. L., Welch, S. K., Klebl, F., Gilbert, T., Seidel, P., Grant, F. J., O'Hara, P. J. and MacKay, V. L. (1994). Cloning and analysis of the Saccharomyces cerevisiae MNN9 and MNN1 genes required for complex glycosylation of secreted proteins. *Proc. Natl. Acad. Sci.* **91**, 2723–2727.